PHYSICAL REVIEW B, VOLUME 63, 115409

Self-limiting growth of transition-metal fluoride films from the reaction with XeF_2

S. R. Qiu and J. A. Yarmoff*
Department of Physics, University of California, Riverside, Riverside, California 92521
(Received 14 August 2000; published 27 February 2001)

Metal-fluoride thin films were grown by reacting XeF_2 with polycrystalline vanadium, iron, and copper surfaces at room temperature. X-ray photoelectron spectroscopy was used to ascertain that films of VF_3, FeF_2, and CuF_2 form on the respective substrates. The film growth initially follows the Mott-Cabrera rate law, but then levels off after a self-limiting thickness is attained. The sudden stop in film growth is attributed to the inability of the precursor molecule to dissociate at the surface when the insulator film becomes too thick for electrons from the substrate to transport through. Thicker films grow on iron and vanadium than on copper, which is attributed to different densities of states at the Fermi level.

DOI: 10.1103/PhysRevB.63.115409 PACS number(s): 81.65.Mq, 82.80.Pv, 73.50.Gr

I. INTRODUCTION

The fundamental aspects underlying the oxidation of metals have been studied extensively because of their importance in the corrosion and protection of metals.[1,2] In comparison to oxygen-containing oxidants, fluorine-related compounds have attracted very little attention, however. The lack of detailed work in metal fluorination is partly related to the corrosive nature of gaseous fluoride compounds, which are hazardous both to humans and to analytical instruments,[3] as well as to the fact that many metal fluorides are volatile. Although the fluorination of semiconductor surfaces has been studied in detail, because of the need to understand the fundamental aspects of dry etching,[4,5] little is known about fluoride formation involving the first row transition metals.[6]

In this paper, metal fluoride thin films are grown by a self-limiting surface oxidation reaction. This work not only serves as a model in the understanding of metal fluoride film growth under controlled conditions, but also furthers the knowledge of the oxidation of metals in general. In addition, transition-metal compounds, such as vanadium fluoride, iron oxide, and copper fluoride, have unique electronic and magnetic properties that can be utilized for catalysis and as magnetic storage media. Thus there is a great interest in developing methods for their synthesis that can be easily adapted to dry processing technology.

It has been widely accepted that the oxidation of metals, and the subsequent growth of metal oxide thin films, can be described by the Mott-Cabrera mechanism. In this mechanism, the dissociation of the oxygen molecules is assumed to be fast, and ion diffusion through the film is the rate-limiting step. Either anions[7,8] or cations[9] can dominate the diffusion process. The driving force for the diffusion of ions is the electric field set up by the surface anions. This mechanism leads to a parabolic rate law for film growth.[10]

In our earlier study, a new observation in the growth of metal fluoride films from fluorine-containing precursor molecules was reported.[7] Films of FeF_2 were grown via a self-limiting process from the reactions of XeF_2 and SeF_6 with atomically clean Fe surfaces in ultra-high vacuum (UHV). The initial film growth rate follows Mott-Cabrera kinetics, but then levels off after reaching a critical thickness. The sudden stop in film growth is due to the inability of the precursor to dissociate at the surface when the insulator film is too thick to enable electron transport from the substrate to the molecule. The ultimate thickness of the films grown from the reaction with XeF_2 is twice that produced from SeF_6. The difference in film thickness for the two reactants suggested that SeF_6 needs to approach the metal substrate more closely than does XeF_2 in order to dissociate.[7]

In the present study, the investigation of the fluorination of transition metals and the growth of metal fluoride films is extended to V and Cu substrates. V, like Fe, is a highly reactive transition metal, while Cu is a noble, or less reactive, metal. A comparison of the behavior of these dissimilar materials provides a more detailed understanding of the growth mechanism. The fluorination of V is also useful as a check of the conclusions drawn in Ref. 7 from the fluorination of Fe. The atomically clean surfaces were exposed to XeF_2 at room temperature and analyzed by x-ray photoelectron spectroscopy (XPS). It is found that VF_3 and CuF_2 films are grown via a similar self-limiting mechanism as was found for FeF_2.[7] Differences in the shutdown thickness are observed between V, Fe, and Cu, which can be related to the densities of states at the Fermi level. The fact that nanometer thick insulator films grow on metal substrates suggests that defects in the films assist the electron transport. The presence of defects, such as grain boundaries and vacancies, creates accessible states in the energy gap that would be absent in a perfect insulator.

II. EXPERIMENTAL PROCEDURE

The experiment was performed in a multichamber UHV system, which consists of a main analysis chamber and a small turbomolecular pumped dosing chamber. Details of this system are described elsewhere.[7,11,12] The sample was transferred under UHV from the dosing chamber to the main chamber after each exposure. All exposures and measurements were performed with the sample at room temperature.

Unmonochromatized Mg $K\alpha$ was used as the XPS radiation source. Binding energies of the photoelectrons were calibrated by linearly fitting the relation between the reported binding energies of clean Fe, Cu, W, Pt, and the measured kinetic energies. All XPS spectra, unless otherwise specified,

 ©2001 The American Physical Society

were collected with the surface normal directed towards the analyzer.

Each foil sample ($8\times8\times0.1\,\mathrm{mm}^3$) was degreased with solvents prior to insertion into the UHV chamber. The surfaces were then cleaned *in situ* by sputtering with 1-keV Ar^+ ions at an ion current density of $\sim1\ \mu\mathrm{A\,mm}^{-2}$ for 3–4 h. Fe and Cu were cleaned at room temperature, and no impurities were detectable by XPS after sputtering. V was sputtered at 400 °C, however, in order to efficiently remove oxygen.[13] Trace amounts of oxygen were inevitably present on the V surface, nevertheless, although two 3-h cycles of sputtering were performed. This amount of oxygen was not sufficient to affect any of the results or conclusions presented here, however.

Exposure to XeF_2 was accomplished by back filling the dosing chamber with XeF_2 through a sapphire leak valve. A 2-mm diameter Cu dosing tube was used to guide the reactant to the sample. XeF_2 was stored in a cylindrical ampule attached to the leak valve. The reactant was purified by three cycles of freeze pumping with liquid N_2, followed by three cycles of freeze pumping with dry ice.

There is a possibility that volatile metal fluorides, formed by the reaction of XeF_2 with metal components in the dosing chamber, could contaminate the sample. Thus care has been taken to guard against this. First, the pressure in the dosing chamber was monitored by a cold-cathode ion gauge in order to prevent any reaction between XeF_2 and the hot filament of a conventional ion gauge. Next, the dosing chamber was exposed to 1.0×10^{-4} Torr of XeF_2 for 30 min prior to introduction of the sample in order to passivate any wall reactions. Note that the pressure measurements were not corrected for sensitivity, and all exposures are reported in langmuirs (L, $1\ \mathrm{L}=10^{-6}$ Torr s).

III. CHEMICAL STATE IDENTIFICATION

Characteristic features in XPS spectra, such as the binding energy of a core level component and its associated satellite features, can be used to ascertain the oxidation state distribution of surface species. Following reaction with XeF_2, the chemical states of the metal fluoride compounds on the surface were discerned by analyzing the primary and secondary features in the V, Fe, and Cu core level spectra.

Four possible oxidation states are available for V when it is fluorinated in UHV. This includes three of the four stable vanadium fluoride compounds, VF_2, VF_3, and VF_4. The fourth stable compound, VF_5, is a liquid at room temperature, and would therefore not remain on the surface in vacuum.[14] The other possible surface species is VF, i.e., a single fluorine atom could attach at each V surface site. After vanadium metal was exposed to XeF_2, the surface reaction products were identified from V $2p$ spectra, such as those shown in Fig. 1. The binding energies of the V $2p_{3/2}$ core level components are summarized in Table I. The metal V $2p_{3/2}$ component has a binding energy of 512.0 eV. Following exposure, a new component emerges at 518.6 eV. The component is first visible after 100 L, but becomes dominant following larger exposures. The increase in intensity of this component and the simultaneous decrease in the metal component intensity with XeF_2 exposure indicate that a metal fluoride film is forming on the metal substrate. For reasons discussed below, we assign this component to VF_3.

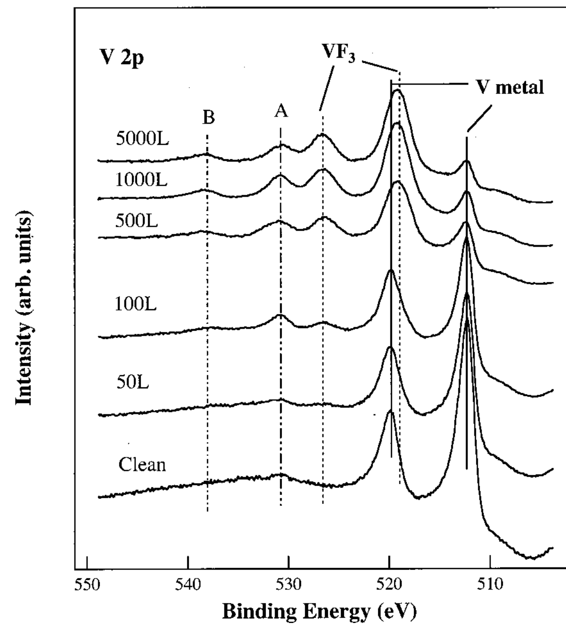

FIG. 1. Representative V $2p$ spectra collected from a sputter cleaned V foil, and from the foil after various exposures to XeF_2.

To further explore the surface chemistry of the vanadium fluoride films, and as an aid in assigning the core-level components, a surface that was exposed to 1000 L of XeF_2 was post annealed at a series of temperatures, each for 90 s. The V $2p$ spectra collected after each annealing are shown in Fig. 2. The intensity of the VF_3 component decreased as the annealing temperature increased, and it completely disappeared after the sample was heated to 600 °C. Another component emerged at 515.2 eV after the film was annealed at ~200 °C. This new, lower binding component reached a maximum intensity at ~350 °C and decreased after the surface was heated to higher temperatures. It is believed that at ~350 °C, the VF_3 overlayer is completely converted to a reduced fluoride. Since its binding energy is lower than that of the original film, but still higher than that of V metal, the reduced fluoride is most likely VF_2. At maximum, the VF_2 film is

TABLE I. Core-level binding energies of several components (in eV).

		$2p_{3/2}$	$3p$	$3s$	Satellites $2p_{3/2}$	Satellites $2p_{1/2}$
	V metal	512.0	36.8	65.6		
V	VF_2	515.2	38.9	67.4		
	VF_3	518.6	42.6	70.3	530.6	538.1
Fe	Fe metal	706.8	52.8			
	FeF_2	711.6	55.9			
Cu	Cu metal	932.7				
	CuF_2	936.4			943.3	962.9

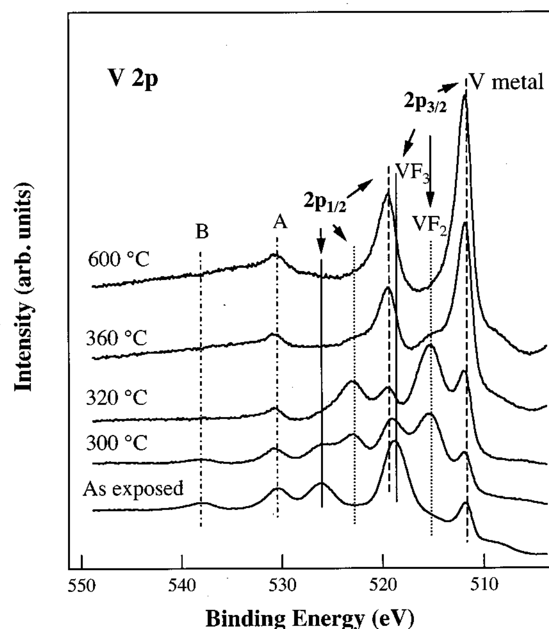

FIG. 2. Representative V $2p$ spectra collected after 90-s anneals of a V foil that had been exposed to 1000 L of XeF_2.

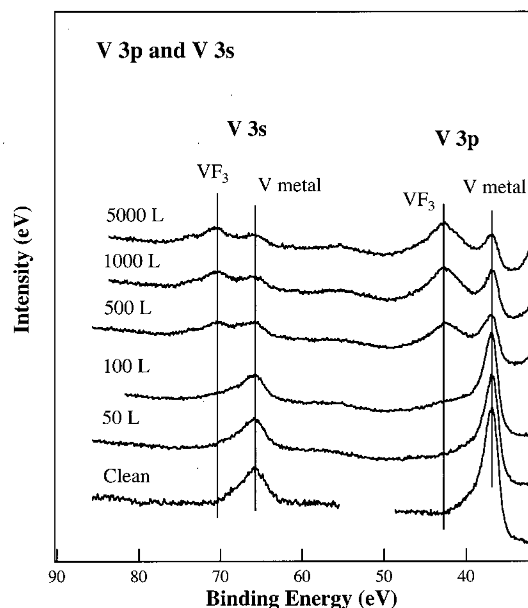

FIG. 3. Representative V $3s$ and $3p$ spectra collected from a sputter cleaned V foil, and from the foil after various exposures to XeF_2.

~40 Å thick, as determined by the method described below. Although radical species, such as VF, could be adsorbed in a stable configuration on the surface, it is difficult to correlate a 40-Å thickness with a structure in which all of the fluorine was singly coordinated.

There are two additional features that appear in the V $2p$ spectra collected after exposures of 100 L and more, which are labeled A and B. The apparent binding energies of these features are given in Table I. The separation between features A and B is ~7.5 eV, which is close to the spin orbit splitting of V $2p$, which could imply that they represent a third XPS component that arises from a new type of vanadium fluoride. This is unlikely, however, as the binding energy shift of ~26 eV from the metal component is unphysical large. A more reasonable explanation is that they are shakeup satellites. Spectra collected after annealing show that features A and B follow the intensity trends of the VF_3 component, which strongly suggests that they are indeed associated with the presence of VF_3. Note that a satellite located ~12 eV below the VF_3 $2p_{3/2}$ component was previously observed in XPS spectra collected from VF_3, which confirms that the film is indeed composed of VF_3.[15] Note that for VF_4, a satellite feature was found at ~15 eV above the $2p_{3/2}$ component.[15] The lack of such a satellite is an indication that VF_4 is not produced by this reaction. Feature B with binding energy of 538.1 eV is possibly another satellite feature associated with VF_3 that was not reported in Ref. 15. Feature A has an additional contribution from O $1s$. This is evident from the spectra shown in Fig. 2. The intensity of feature A decreased after the first heating, but then increased again when the sample was heated at higher temperatures. The spectral line is also broadened with temperature, and the peak position shifted by 0.3 eV. The changes seen for feature A can be attributed to a combination of the desorption of F and the contamination by oxygen as the temperature is raised. Two possible sources of oxygen contamination are consistent with an increase in the O $1s$ intensity at higher temperatures. One is diffusion of oxygen from the bulk,[13] and the other is adsorption of oxygen produced by outgasing of the sample holder.

To further support the assignments made here, V $3s$ and V $3p$ spectra were collected after each exposure. Representative spectra are shown in Fig. 3. The clean surface spectra show only a single component for both levels, as the $3p$ spin-orbit splitting is too small to resolve. After a 100-L exposure, new components appear at a higher binding energy than the metal component in both the V $3s$ and V $3p$ spectra. The intensities of the new components increase with exposure, while the metal component intensities decrease. No other components are apparent at any other exposure level. This confirms that only one type of vanadium fluoride is formed via reaction with XeF_2 at room temperature, and thus supports the notion that features A and B arise from satellites.

The stable iron fluorides that exist in nature are FeF_2 and FeF_3, both of which possess high melting temperatures.[14] The formation of FeF_2 by the reaction of Fe with XeF_2 was reported in Ref. 7. Representative Fe $2p$ spectra collected after exposure are shown in Fig. 4. For the current work, additional spectra were collected following the annealing of a surface that had been reacted with 1000 L of XeF_2, which are also included in Fig. 4. The binding energy of the shifted component in the as-grown spectra shows that the main iron fluoride species is FeF_2. When the film is heated, the intensity of the FeF_2 component decreases due to thermal desorption of F and no new species are formed. After a 450 °C anneal, all of the F is removed from the surface.

A single phase of CuF_2 was formed after the reaction of

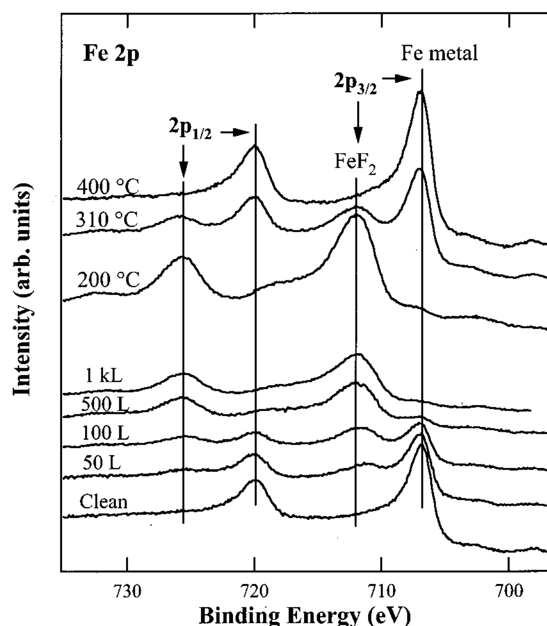

FIG. 4. Representative Fe $2p$ spectra collected from a sputter cleaned Fe foil, from the foil after various exposures to XeF_2, and after 90-s anneals of an Fe foil that had been exposed to 1000 L of XeF_2.

Cu foil with XeF_2, as evident in the representative Cu $2p$ spectra shown in Fig. 5. Although both CuF and CuF_2 are stable, and an earlier study did show that CuF forms when a Cu surface heated to ~900 K is exposed to F_2 gas in UHV,[16] only CuF_2 is apparent here. There are two components in the spectra, one is from the Cu metal and the other is from a Cu fluoride. The binding energies of these components are listed in Table I. Satellite features relating directly to Cu (II) ion are clearly visible in the spectra with one peak at 6.4 eV from Cu (II) $2p_{1/2}$ and another at 6.9 eV from Cu (II) $2p_{3/2}$. These features and peak positions were reported previously,[17–19] and indicate that the metal fluoride formed is indeed CuF_2. When the film was heated, no CuF was formed, but F desorbed from the surface reducing the intensity of the CuF_2 component. After heating to 350 °C, all of the F was removed from the surface and the spectrum that was obtained was identical to that collected after sputter cleaning.

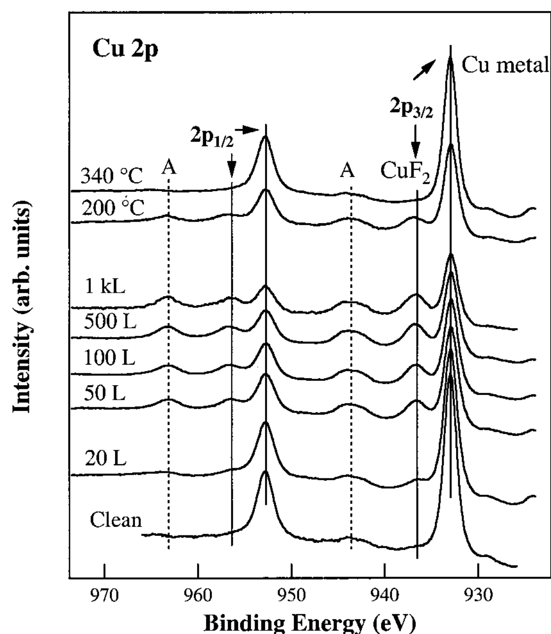

FIG. 5. Representative Cu $2p$ spectra collected from a sputter cleaned Cu foil, from the foil after various exposures to XeF_2, and after 90-s anneals of a Cu foil that had been exposed to 1000 L of XeF_2.

IV. FILM THICKNESS DETERMINATION

In order to obtain quantitative information, V $3p$, Fe $3p$, and Cu $2p$ core-level spectra were curve fit with Gaussian-Lorentzian sum functions. For all of these metals, the $2p$ spectra have very complicated satellite structures, large spin-orbit splittings, and complex secondary electron backgrounds.[17,19,20] These complications make it difficult to model the backgrounds and fit the $2p$ spectra. V $3p$ and Fe $3p$, on the other hand, have a much simpler background structure due to their high kinetic energies, negligible spin-orbit splittings, and negligible satellite features. Although the $3p$ levels are less intense than the $2p$ levels, there is sufficient signal to use them here. Since Cu $3p$ has a much larger spin-orbit splitting than V $3p$ and Fe $3p$, the $2p$ level was used for Cu, although only the $2p_{3/2}$ component was actually fit in order to reduce the complications that arise from the secondary structures.

Representative V $3p$ spectra collected after exposure are shown along with numerical fits in Fig. 6. The photoelectron background was modeled with the Shirley method.[21] The binding energy, peak width, Gaussian-Lorentzian ratio, and asymmetry parameters for the substrate V $3p$ component were determined from a spectrum collected from the clean surface, and then kept constant in fitting the spectra collected from the reacted surfaces. The fluoride component was fit with different parameters than the bulk. The final set of fitting parameters for the fluoride component was checked for consistency throughout all of the spectra. The bulk component at 36.9 eV is consistent with the reported value for clean V metal.[22] The second component with a binding energy of 42.6 eV is assigned to VF_3. Note that representative fits of Fe $3p$ spectra collected after reaction with XeF_2 are shown in Ref. 7.

Thicknesses of the thin metal fluoride films were determined from the intensity ratios of the metal fluoride core-level component to that of the bulk metal. Since the same core level was used for both the substrate and overlayer, differences in the instrumental response of the photoelectrons emitted from the two components can be ignored. Several assumptions were also made in the calculation. First, that a homogeneous halide film is grown on the metal substrate and that there is a sharp interface between them. Second, that the photoionization cross sections and the electron inelastic mean free paths are the same for both the substrate

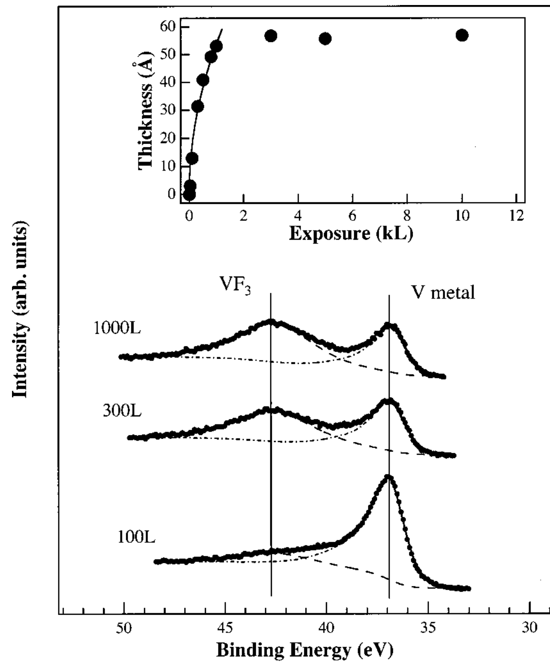

FIG. 6. Representative V $3p$ spectra are shown along with numerical fits to the data for V foil following reaction with XeF_2. The raw data are denoted by filled circles, dashed lines indicate the individual components of the fits, and solid lines show the sums of the fit components. The inset shows the thickness of VF_3 plotted as a function of exposure. The initial portion of the film growth is modeled by a parabolic function, which is indicated by the solid line.

and the metal fluoride. The limitations of these assumptions contribute a very small error in the calculated thickness.[7,11,12] The formula used in the calculation is[12]

$$d=\lambda \cdot \ln\left(1+\frac{\rho_s}{\rho_a}\frac{M_a}{M_s}\frac{I_a}{I_s}\right). \tag{1}$$

In this equation, the subscript a refers to the overlayer, while s refers to the substrate. I is the intensity of the relevant component, ρ is the density of the bulk compound, M is the molecular weight, d denotes the film thickness, and λ is the electron inelastic mean free path (IMFP). The IMFP was determined by the method described in Refs. 23 and 24.

The calculated thicknesses of the VF_3 films produced by the reaction with XeF_2 are plotted as a function of exposure in the inset to Fig. 6. It is seen that the film thickness initially increases rapidly with exposure and then levels off at ~1000 L, after which no further increase is observed. The film thicknesses below 1000 L can be fit very well to a parabolic function, as shown by the solid line in the inset. This indicates that the initial growth follows a Mott-Cabrera mechanism. It was not possible, however, to fit the entire set of data to a single parabolic function. Similar film growth behavior was reported earlier for iron fluoride films grown from XeF_2 and SeF_6.[7,12] The sudden stop in film growth was attributed to the inability of the molecules to dissociate when they are too far from the metal substrate.

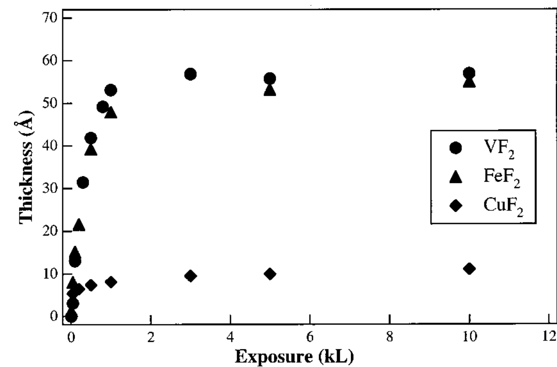

FIG. 7. The thicknesses of VF_2, FeF_2, and CuF_2 films are shown as a function of exposure to XeF_2.

The growth rates of the various metal fluoride films vs exposure are compared in Fig. 7. The ultimate thicknesses are similar for VF_3 and FeF_2, at ~55 Å, but much smaller for CuF_2, at ~10 Å. For all of these films, the initial growth can be modeled very well by a parabola, although the proportionality constants are different for each material. It is impossible, however, to fit the entire exposure range to a single parabolic function for any of the materials.

V. DISCUSSION

The film growth process takes place through a number of steps that include the dissociation of the precursor molecule, anion formation, and ion diffusion through the insulator film. Any of these steps could be rate limiting. In the oxidation of metals at high temperature by O_2, ion diffusion is the dominant limiting factor, while the dissociation of the reactant molecule is not.[25] The growth of such metal oxide films therefore follows the Mott-Cabrera model, and the growth rate is a parabolic function for all exposures. In the present study, Mott-Cabrera oxidation is also observed during the initial stages of film growth on Fe, V, and Cu metals. However, after a critical thickness is reached, the growth is quenched. This sudden stop in film growth suggests that another limiting factor has become involved. This is presumably the dissociation of XeF_2 precursor molecule at the surface, as was proposed in Ref. 7 for the growth of FeF_2 from XeF_2 and SeF_6. If the precursor molecule is unable to dissociate, the production of atomic F ceases, which causes the film growth to stop.

When a molecule approaches a metal surface, it first physisorbs into a long-lived precursor state. While physisorbed, the molecular orbitals rearrange accordingly due to the effects of the image charge potential.[6,26] When the antibonding orbitals bend down below the metal Fermi level, electrons from the metal substrate can harpoon to the molecule and fill the empty molecular states. The molecule is thus driven into an excited state, from which it subsequently dissociates.[6,27,28] Following dissociation, the atomic F picks up another electron resonantly to become F^-, since the affinity level of F is positioned below the Fermi level when the atom is close to the surface.[29–31] This negative ion then participates in film growth via Mott-Cabrera diffusion.

At the initial stages of the film growth, i.e., while the metal surface is covered with less than a monolayer of FeF_2, the electrons that are needed to initiate dissociation can tunnel directly from the substrate. When the film becomes thicker, however, it is less likely that electrons can quantum mechanically tunnel through the insulator layer. A simple calculation was employed to illustrate this point, in which the electron tunneling coefficient through a square energy barrier was estimated. In this model, the electron tunneling probability is an exponential function of the barrier width,[32] and also depends on the work function of the material and the energy of the electrons. To model the electrons needed for dissociation of XeF_2 at the surface, the work function was assumed to be 5 eV and the electrons were assumed to be at the Fermi level. The calculation predicted that any thickness in excess of 1–2 Å will prevent an appreciable number of electrons from tunneling to a molecule at the surface. Since nanometer-thick insulator films were grown via surface reaction, electrons must have utilized means other than tunneling to transport through the film in order to initiate dissociation.

In a perfect insulator, there is a large energy gap between the conduction band and valence band in which no accessible electronic states are available. However, it is likely that the materials produced in the present work are not ideal in that gap states exist due to the presence of defects, such as vacancies or grain boundaries. Conduction electrons from the high-energy tail can occupy these states by direct tunneling. Electrons can then hop from state to state in order to transport through the insulator film. For strongly localized defects, electron-phonon interactions can be strong,[33] and the electrons captured in defect sites can be reemitted by absorbing phonons.[34] Defect-enhanced low energy electron transport through semiconductors and insulators has been observed in other studies.[33,35]

As long as electrons can travel to the surface of the overlayer, there is finite probability that an electron will tunnel to the XeF_2 molecule and initiate the dissociation. The self-limiting thickness of the metal fluoride film thus corresponds to the thickness at which the probability for electrons to travel through the film reduces to zero. In order for the electron transport to diminish with thickness, the defect density must decrease as the film grows. For example, fluorine vacancies in the film can be tied up by additional fluorine atoms as the reaction with XeF_2 progresses, which would reduce the number of vacancy defects with increasing thickness. Or, if electron transport occurs along grain boundaries, then the probability that a single boundary can cover the distance from the interface to the surface decreases with film thickness.

The reactivity of metals and alloys is intimately related to the valence-band structure, since the electrons at the Fermi energy are responsible for heterogeneous reaction at an interface.[36] A comparison of the valence bands of these metals reveals a possible explanation of the difference in thickness of the metal fluoride films. V and Fe have nearly identical large and broad densities of states (DOS) at E_f.[37] Cu, however, has a relatively low DOS at E_f, and a dominant *d*-electron feature at ~3 eV below E_f.[38,39] The low DOS at E_f is responsible for the noble metal nature of copper. Since both V and Fe have similar electronic structures around E_f, it is not surprising that they produce a comparable overlayer thickness when reacted with XeF_2. There are far fewer electrons available to dissociate a molecule at the surface of Cu, however, which explains the relatively small thickness of the CuF_2 films.

VI. CONCLUSIONS

The reactions of XeF_2 with V, Fe, and Cu transition metals were investigated by XPS. Films of VF_3, FeF_2, and CuF_2 are grown by the reaction. When a reacted V surface is annealed to 300 °C, it converts to VF_2, which indicates that there is a high energy barrier for the formation of VF_2. These results suggest a better approach for the synthesis of VF_2 thin films.[40,41] Furthermore, they suggest that Cu metal can be used in a storage container for F-containing compounds, as a thin CuF_2 protective layer readily forms.

Metal fluoride film growth from XeF_2 at room temperature initially follows Mott-Cabrera kinetics, in which the diffusion of ions is the rate-limiting step. The growth suddenly stops, however, after a self-limiting thickness is reached. Defects in the insulator films play a critical role in the dissociation of the precursor molecule by assisting electrons transport. V and Fe produce much thicker films than Cu, due to the different valence-band structures of these metals. This work suggests a new approach for the growth of thin films on metal substrates by a self-limiting chemical process that uses molecular precursors.

ACKNOWLEDGMENTS

The authors are grateful for support from the U.S. Department of Energy Environmental Management Science Program (DE-FG07-96ER14707). S.R.Q. acknowledges support from the National Science Foundation IGERT program (DGE-9554506).

*Corresponding author. Email address: yarmoff@ucr.edu

[1] J. C. Scully, *The Fundamentals of Corrosion* (Pergamon, New York, 1990).
[2] J. A. T. Fromhold, *Theory of Metal Oxidation* (North-Holland, New York, 1976).
[3] E. Bechtold and H. Leonhard, Surf. Sci. **151**, 521 (1985).
[4] H. F. Winters and J. W. Coburn, Surf. Sci. Rep. **14**, 161 (1992).
[5] W. C. Simpson and J. A. Yarmoff, Annu. Rev. Phys. Chem. **47**, 527 (1996).
[6] P. A. Dowben, CRC Crit. Rev. Solid State Mater. Sci. **13**, 191 (1987).
[7] S. R. Qiu, H.-F. Lai, and J. A. Yarmoff, Phys. Rev. Lett. **85**, 1492 (2000).
[8] H. D. Ebinger and J. T. Yates, Jr., Phys. Rev. B **57**, 1976 (1998).
[9] R. J. Friauf, J. Appl. Phys. **33**, 494 (1962).
[10] N. Cabrera and N. F. Mott, Rep. Prog. Phys. **12**, 163 (1948).

[11] S. R. Qiu, H.-F. Lai, M. J. Roberson, M. L. Hunt, C. Amrhein, L. C. Giancarlo, G. W. Flynn, and J. A. Yarmoff, Langmuir **16**, 2230 (2000).
[12] S. R. Qiu, H.-F. Lai, H. T. Than, C. Amrhein, and J. A. Yarmoff Surf. Sci. **462**, 17 (2000).
[13] C. M. Kim, B. D. D. Vries, B. Fruhberger, and J. G. Chen, Surf. Sci. **327**, 81 (1995).
[14] *Handbook of Chemistry and Physics*, edited by D. R. Lide (CRC, New York, 1995).
[15] G. A. Vernon, G. Stucky, and T. A. Carlson, Inorg. Chem. **15**, 278 (1976).
[16] K. Sugawara, T. Wach, J. Wanner, and P. Jakob, J. Chem. Phys. **102**, 544 (1995).
[17] D. C. Frost, A. Ishitani, and C. A. McDowell, Mol. Phys. **24**, 861 (1972).
[18] S. W. Gaarenstroom and N. Winograd, J. Chem. Phys. **67**, 3500 (1977).
[19] R. P. Vasquez, Surf. Sci. Spectra **2**, 155 (1994).
[20] Y. Gao, Y. J. Kim, and S. A. Chambers, J. Mater. Res. **13**, 2003 (1998).
[21] D. A. Shirley, Phys. Rev. B **5**, 4709 (1972).
[22] D. Vaughan, *X-ray Data Booklet* (Lawrence Berkeley Laboratory, Berkeley, CA, 1986).
[23] C. J. Powell, A. Jablonski, I. S. Tilinin, S. Tanuma, and D. R. Penn, J. Electron Spectrosc. Relat. Phenom. **98-99**, 1 (1999).
[24] NIST Electron Inelastic-Mean-Free-Path Database, Standard Reference Data Program 71, 1999.
[25] S. R. J. Saunders, Sci. Prog. **63**, 163 (1976).
[26] A. Zangwill, *Physics at Surfaces* (Cambridge University Press, New York, 1988).
[27] C. W. Lo, Ph.D. dissertation (Department of Physics, University of California, Riverside, CA, 1993).
[28] *Comprehensive Inorganic Chemistry*, edited by J. C. Bailar, H. J. Emeleus, S. R. Nyholm, and A. F. Trotman-Dickenson (Pergamon, Oxford, 1973).
[29] C. G. Van-der-Walle, F. R. McFeely, and S. T. Pantelides, Phys. Rev. Lett. **61**, 1867 (1988).
[30] H. F. Winters and D. Haarer, Phys. Rev. B **36**, 6613 (1987).
[31] Y. E. Babanov, A. V. Prokaznikov, and V. B. Svetovoy, Vacuum **41**, 902 (1990).
[32] J. A. Kubby and J. J. Boland, Surf. Sci. Rep. **26**, 61 (1996).
[33] L. E. Mir and C. Bourgoin, Phys. Status Solidi B **207**, 577 (1998).
[34] E. M. Korol, Fiz. Tverd. Tela (Leningrad) **19**, 2266 (1977) [Sov. Phys. Solid State **19**, 1327 (1977)].
[35] E. Cartier and P. Pfluger, Appl. Phys. A: Solids Surf. **44**, 43 (1987).
[36] S. V. Didziulis, Langmuir **11**, 917 (1995).
[37] L. Ley, O. B. Dabbousi, S. P. Kowalczyk, F. R. McFeely, and D. A. Shirley, Phys. Rev. B **16**, 5372 (1977).
[38] P. Pervan, T. Valla, and M. Milun, Surf. Sci. **397**, 270 (1998).
[39] P. Pervan, T. Valla, and M. Milun, Vacuum **50**, 245 (1998).
[40] J. W. Stout and W. O. J. Boo, J. Appl. Phys. **37**, 966 (1966).
[41] M. W. Shafer, Mater. Res. Bull. **4**, 905 (1969).